PREDICTING REACHING POSTURES USING A KINEMATICALLY CONSTRAINED SHOULDER MODEL

Vincent De Sapio, James Warren, and Oussama Khatib

Artificial Intelligence Laboratory

Stanford University

{vdesap, warren, khatib}@stanford.edu

Abstract   We present a new muscle effort criteria for predicting physiologically accurate upper limb motion in human subjects based on skeletal kinematics, muscle routing kinematics, and muscle strength characteristics. The new criteria properly accounts for the cross-joint coupling associated with the routing kinematics of multi-articular muscles. We also employ a new kinematically constrained model of the human shoulder complex, which is critical for the proper evaluation of our muscle effort criteria. Through a set of subject trials we have shown good correlation between natural reaching postures and our proposed criteria.

Keywords: Muscle effort, shoulder complex, constraints, muscle routing kinematics

1.   Introduction

The prediction and synthesis of human movement has presented a daunting challenge to the biomechanics, neuroscience, and robotics communities. In the presence of this challenge there is a significant motivation to understand and emulate human movement. Given a specific task the prediction of kinematically redundant upper limb motion is a problem of choosing one of a multitude of control solutions which all yield kinematically feasible solutions. It has long been observed that humans resolve this redundancy problem in a relatively consistent manner (Lacquaniti and Soechting, 1982; Kang et al., 2005). For this reason general mathematical models have proven to be valuable tools for motor control prediction across human subjects.

Many of the models for predicting human arm movement, including the minimum work model (Soechting et al., 1995) and the minimum torque-change model (Uno et al., 1989), do not involve any direct inclusion of muscular properties such as routing kinematics and strength properties. Even models described as employing biomechanical variables (Kang et al., 2005) typically employ only variables derivable purely from skeletal kinematics and not musculoskeletal behavior. We feel that the

utilization of a model-based characterization of muscle systems (Zajac, 1993; Delp and Loan, 2000), which accounts for muscle kinematic and strength properties, is critical to authentically simulating human motion since all human motion is rooted in, and bounded by, physiological capabilities.

We will present a new methodology for predicting arm configuration in reaching movements by examining the muscular effort required to perform positioning tasks. This is built upon the work of Khatib et al., 2004, but involves a number of improvements in methodology. An important element of this approach is the implementation of a sufficiently sophisticated musculoskeletal model of the upper limb that accounts for kinematic coupling between the constituents of the human shoulder complex (Holzbaur et al., 2005). This provides fidelity in predicting muscle forces, joint moment arms, and resulting muscle induced joint moments, particularly in the shoulder complex. With our methodology and physiological models we show that natural task-driven human arm postures can be predicted accurately using a criteria based on a skeletal kinematics, muscle routing kinematics, and muscle strength characteristics. This is validated through a set of targeted subject trials.

2.   Human Upper Extremity Model

The upper extremity model of Holzbaur et al., 2005, has been employed, with some modification, in this work. The model, consisting of a shoulder complex and a lower arm, has been implemented in the SIMM (**S**oftware for **I**ntegrated **M**usculoskeletal **M**odeling) environment (Delp and Loan, 2000). A minimal set of 7 generalized coordinates were chosen to describe the configuration of the shoulder complex, elbow, and wrist (3 for the shoulder complex, 2 for elbow flexion and pronation, and 2 for wrist flexion and deviation). This is depicted in Fig. 1.

Fidelity in predicting muscle action was an important requirement for the model employed in this work. In particular, proper kinematics of the shoulder complex is critical in generating realistic muscle paths and associated joint moments. While the purpose of the shoulder complex is to produce spherical articulation of the humerus, the resultant motion does not exclusively involve motion of the glenohumeral joint (see Fig. 1). The shoulder girdle, which is comprised of the clavicle and scapula, connects the glenohumeral joint to the torso and produces some of the motion associated with the overall articulation of the humerus. While this motion is small compared to the glenohumeral motion its impact on overall arm function is significant (Klopčar and Lenarčič, 2001; Lenarčič
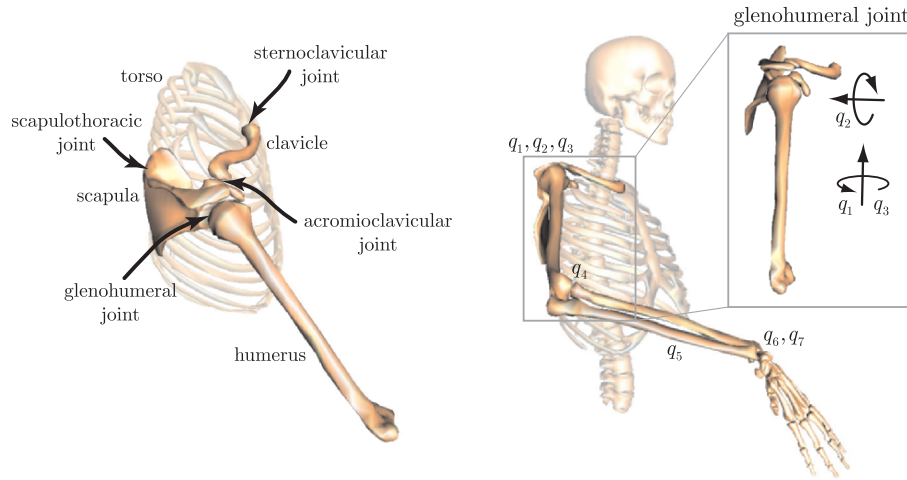
Figure 1. (Left) Constituents of the shoulder complex including the scapula, clavicle, and humerus. The glenohumeral joint produces spherical motion of the humerus. The shoulder girdle attaches the glenohumeral joint to the torso and influences the resultant motion of the humerus. (Right) Kinematic parameterization of the model of Holzbaur et al.

et al., 2000). Part of this impact is related to the shoulder girdle's influence on the muscle routing kinematics.

The constrained movement of the shoulder girdle was determined from the shoulder rhythm regression analysis of de Groot and Brand, 2001. The model obtained from this regression analysis was shown to fit well for an independent set of shoulder motions and on a different set of subjects than was used for the regression analysis. For these reasons the model of de Groot and Brand is considered to be superior in predicting shoulder motion than a simple unconstrained model which only reflects glenohumeral rotation. Using the results of de Groot and Brand the constraints that model the shoulder girdle are implicitly handled, with all motions of the shoulder girdle being dependent on the three glenohumeral rotation coordinates. These are elevation plane, q_1, elevation angle, q_2, and shoulder rotation, q_3.

Due that fact that SIMM restricts any joint motion to a function of a single independent generalized coordinate, the regression equations were simplified by Holzbaur et al. to be a function of only thoracohumeral (humerus elevation) angle, q_2. The shoulder kinematics for this parameterization are shown in Table 1.

The terms d_1, d_2, and d_3 are fixed translation vectors and $Q_1, \cdots, Q_7$ are rotation matrices associated with spins about successive local

Table 1. Shoulder kinematics using a minimal set of generalized coordinates.

Translation	Rotation
clavicle	
${}^t\boldsymbol{d}_c = \boldsymbol{d}_1$	${}^t_c\boldsymbol{Q} = \boldsymbol{Q}_1(c_1 q_2)\boldsymbol{Q}_2(c_2 q_2)$
scapula	
${}^t\boldsymbol{d}_s = {}^t\boldsymbol{d}_c + {}^t_c\boldsymbol{Q}\boldsymbol{d}_2$	${}^t_s\boldsymbol{Q} = \boldsymbol{Q}_3(c_3 q_2)\boldsymbol{Q}_4(c_4 q_2)\boldsymbol{Q}_5(c_5 q_2)$
humerus	
${}^t\boldsymbol{d}_h = {}^t\boldsymbol{d}_s + {}^t_s\boldsymbol{Q}\boldsymbol{d}_3$	${}^t_h\boldsymbol{Q} = \boldsymbol{Q}_6(q_1)\boldsymbol{Q}_7(q_2)\boldsymbol{Q}_6(-q_1)\boldsymbol{Q}_6(q_3)$

coordinate axes, where the arguments identify the spin angles. The super-script t refers to the torso as the frame of reference. The constraint constants, $\boldsymbol{c}$, associated with the dependency on humerus elevation angle, q_2, were obtained from the regression analysis of de Groot and Brand, 2001.

De Sapio et al., 2006, provide an extensive analysis of the impact of shoulder girdle motion, associated with glenohumeral coupling constraints, on the muscle routing kinematics and moment arms about the glenohumeral joint. The constrained model employed here typically generates moment arms of substantially larger magnitude than those of a simple model with no kinematic coupling between glenohumeral and shoulder girdle motion. The resulting moment generating capacities associated with the constrained model are also typically larger in magnitude than those associated with the simple model. This is of paramount importance for the implementation addressed in the following section.

3. Muscle Effort Minimization

A scalar measure of instantaneous (path independent) muscle effort at a specific configuration can be defined based on the necessary gravity torque to maintain the configuration and the muscle strength capacity at the configuration. Activation, which represents the normalized exertion of muscles, provides a natural measure for this. Specifically, the magnitude of the muscle activation vector, $\boldsymbol{a}$, has been used as a scalar optimization criteria in both static and dynamic optimizations. That is, we can choose our instantaneous muscle effort measure, U, to be $U(\boldsymbol{q}, \dot{\boldsymbol{q}}) = \|\boldsymbol{a}\|^2$. To express this measure we first represent the joint torques, $\boldsymbol{\Gamma}$ in terms of muscle action,

$$\boldsymbol{\Gamma}(\boldsymbol{q}, \dot{\boldsymbol{q}}, \boldsymbol{a}) = \boldsymbol{K}_\Gamma(\boldsymbol{q}, \dot{\boldsymbol{q}})\boldsymbol{a} \tag{1}$$

where $\boldsymbol{K}_\Gamma(\boldsymbol{q}, \dot{\boldsymbol{q}})$ is the muscle torque-activation gain matrix. That is, it maps muscle activation, $\boldsymbol{a}$, to joint torque (De Sapio et al., 2005). Due to the fact that there are typically more muscles spanning a set of joints than the number of generalized coordinates used to describe those joints this equation will have an infinite set of solutions for $\boldsymbol{a}$. Choosing the solution, $\boldsymbol{a}_o$, which has the smallest magnitude yields,

$$\boldsymbol{a}_o = \boldsymbol{K}_\Gamma^+ \boldsymbol{\Gamma} = \boldsymbol{K}_\Gamma^T (\boldsymbol{K}_\Gamma \boldsymbol{K}_\Gamma^T)^{-1} \boldsymbol{\Gamma} \tag{2}$$

where $\boldsymbol{K}_\Gamma^+$ is the pseudoinverse of $\boldsymbol{K}_\Gamma$. Our muscle effort measure can then be expressed as,

$$U(\boldsymbol{q}) = \|\boldsymbol{a}_o\|^2 = \boldsymbol{g}^T (\boldsymbol{K}_\Gamma \boldsymbol{K}_\Gamma^T)^{-1} \boldsymbol{g} \tag{3}$$

Note that we have eliminated the dependency on $\dot{\boldsymbol{q}}$, as we will concern ourselves only with static configurations for the remainder of our analysis. Similarly, $\boldsymbol{\Gamma}$ has been replaced with the configuration space gravity vector, $\boldsymbol{g}$, since in the static case $\boldsymbol{\Gamma} \to \boldsymbol{g}$. Expressing this in terms of constituent terms we have,

$$U(\boldsymbol{q}, \dot{\boldsymbol{q}}) = \boldsymbol{g}^T [\boldsymbol{L}^T (\boldsymbol{K}_f \boldsymbol{K}_f^T) \boldsymbol{L}]^{-1} \boldsymbol{g} \tag{4}$$

where we have made use of the relationship, $\boldsymbol{K}_\Gamma = \boldsymbol{L}^T \boldsymbol{K}_f$. The muscle force-activation gain matrix, $\boldsymbol{K}_f$, maps muscle activation to muscle force (De Sapio et al., 2005). The transpose, $\boldsymbol{L}^T$, of the muscle Jacobian is a kinematic quantity, based on muscle routing kinematics, that maps muscle force to joint torque (Khatib et al., 2004). If we dissect the structure of this effort criteria as follows,

$$U = \boldsymbol{g}^T [\underbrace{\overbrace{\underbrace{\boldsymbol{L}^T}_{\text{kinematics}} \underbrace{(\boldsymbol{K}_f \boldsymbol{K}_f^T)}_{\text{kinetics}} \underbrace{\boldsymbol{L}}_{\text{kinematics}}}^{\text{muscular capacity}}]^{-1} \boldsymbol{g} \tag{5}$$

we gain some physical insight into what is being measured. The terms inside the brackets represent a measure of the net capacity of the muscles. This is a combination of the force generating kinetics of the muscles as well as the mechanical advantage of the muscles, as determined by the muscle routing kinematics. The terms outside of the brackets represent the kinetic requirements of the task/posture; in this case the gravity torques at the joints.

Eq. 5 represents a generalization of the joint decoupled measure used by Khatib et al., 2004. That measure projected muscle strength capacities to the joint level in a decoupled manner. Consequently, the cross-joint coupling associated with multi-articular muscles (muscles that span

more than one joint) was ignored. The measure of Eq. 5 properly accounts for multi-articular muscle coupling in the musculoskeletal system.

It is noted that the solution of Eq. 1 expressed in Eq. 2 corresponds to a constrained minimization of $\|\boldsymbol{a}\|^2$, however, this solution does not enforce the constraint that muscle activation must be positive (muscles can only produce tensile forces). Imposing the inequality constraint, $a \geqslant 0$, on the activations requires a quadratic programming approach to performing the constrained minimization. In this case the solution to Eq. 1 which minimizes $\|\boldsymbol{a}\|^2$ and satisfies $a \geqslant 0$ can be represented in shorthand as,

$$\boldsymbol{a}_o = \mathrm{qp}(\boldsymbol{K}_\Gamma, \boldsymbol{\Gamma}, \|\boldsymbol{a}\|^2, \, a_i \geqslant 0) \tag{6}$$

where $\mathrm{qp}(\cdot)$ represents the output of a quadratic programming function (eg. `quadprog()` in the Matlab optimization toolbox). Our muscle effort criteria is then $U(\boldsymbol{q}) = \|\boldsymbol{a}_o\|^2$, where $\boldsymbol{a}_o$ is given by Eq. 6. Despite the preferred use of quadratic programming for computational purposes, Eq. 5 provides valuable insights at a conceptual level.

To find a task consistent static configuration which minimizes $U(\boldsymbol{q})$, we first define the self-motion manifold associated with a fixed task point, $\boldsymbol{x}_o$. This is given by $M(\boldsymbol{x}_o) = \{\boldsymbol{q} \,|\, \boldsymbol{x}(\boldsymbol{q}) = \boldsymbol{x}_o\}$ where $\boldsymbol{x}(\boldsymbol{q})$ is the operational point of the kinematic chain (e.g. the position of the hand). The problem of finding a minimal effort task consistent configuration can then be stated as minimizing $U(\boldsymbol{q})$ on $M(\boldsymbol{x}_o)$.

4. Experiments

A set of experiments was conducted to provide validation for the muscle effort minimization approach of Section 3. The subjects chosen were six right-handed adult males with normal or corrected-to-normal vision. The subjects were seated with a test fixture directly in front of them. The test fixture contained five visual targets represented as physical markers positioned at different locations. A set of weights (5, 8, and 15 lbs) were placed to the side of the subjects. An eight-camera Qualisys retroreflective motion capture system was used to record subject motion during the trials at a capture rate of 250 Hz.

The subjects performed a set of tasks designed to isolate upper limb reaching motion. While seated each subject was instructed to pick up a weight and move it to each target and hold a static configuration at the target for 4 seconds (see Fig. 2). The subjects were instructed to perform the movement in any manner which felt natural and comfortable to them. Five consecutive trials were performed for each weight (8, 12, and 15lb) as well as a trial with no weight in hand, for a total of 20

trials. The total number of 20 trials took each subject roughly an hour to perform; including time for hardware set up and marker placement.
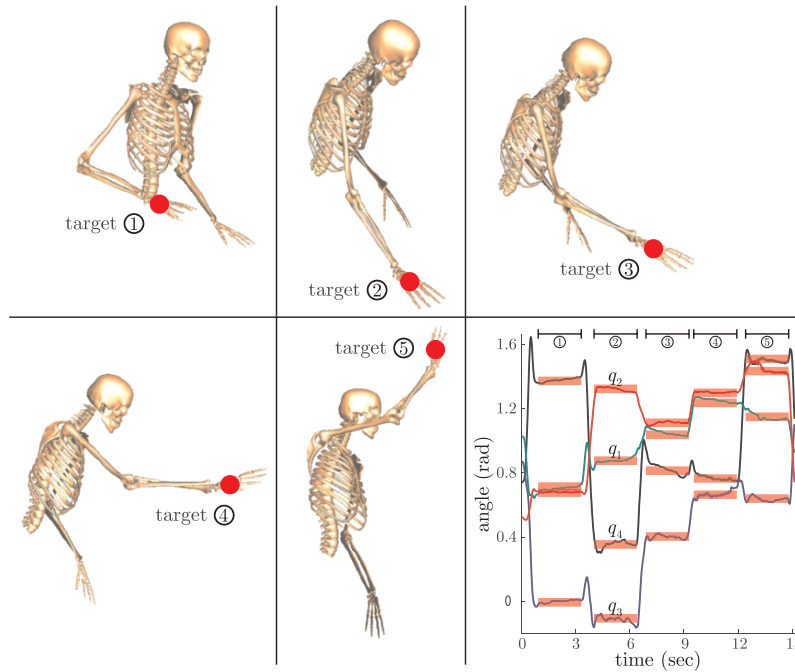

Figure 2. Subject reaching to a set of 5 target locations from a seated configuration. The subject performs these targeted reaching movements freehand and with a total of three different weights in hand. Time histories of shoulder joint angles, q_1, q_2, and q_3, and elbow joint angle, q_4, show steady state configurations at each of the targets.

Following motion capture the marker data was segmented using the Qualisys Track Manager software. To obtain joint space trajectories, custom Matlab scripts were written based on the inverse kinematics of the constrained shoulder complex presented in Section 2. The steady state configurations associated with the five targets were obtained from the joint space trajectories for each trial (see Fig. 2). For each configuration a 1-dimensional self motion manifold, $M(\mathbf{x}_o)$, was computed numerically given the fixed target location, $\mathbf{x}_o$. The manifold was associated with the variation of the 3 shoulder complex joint angles, q_1, q_2, and q_3, and the elbow joint angle, q_4.

The muscle effort criteria of Section 3 was then computed. SIMM was used to generate the maximum muscle induced moments over the self motion manifold for each trial. Matlab scripts were then written to construct the muscle torque-activation gain matrix, $\mathbf{K}_\Gamma$, from the computed muscle moments as well as the gravity vector, $\mathbf{g}$. A quadratic

programming routine (`quadprog()` from Matlab's optimization toolbox) was used to enforce positive values for muscle activation.

Figure 3 depicts the results of the muscle effort computations for one of the subject trials with no weight in hand. The subject's chosen configuration was typically within several degrees (norm based metric along the self motion manifold) of the predicted configuration associated with minimizing the computed muscle effort. This was consistent across the set of subjects, with the largest deviation between experimental and predicted configurations being on the order of 25° and more commonly under 10°.
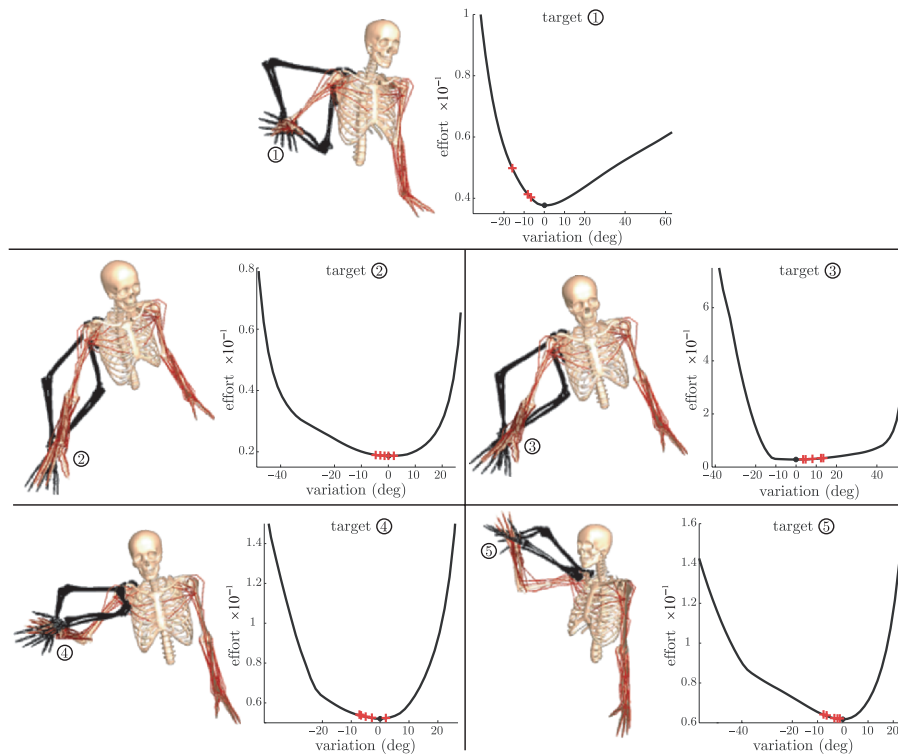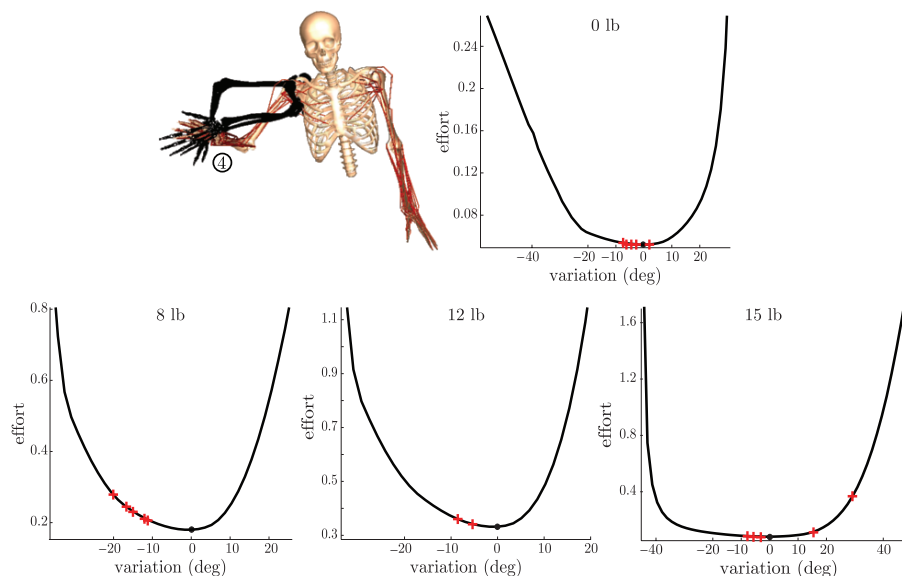

Figure 3.   Muscle effort variation for one of the subject trials with no weight in hand. Each plot depicts the muscle effort for one of the five target configurations. The locations of the subject's chosen configurations are depicted with a red +. The full range of motion is depicted by the black silhouettes (±90° from nominal).

Figure 4 depicts the results of the muscle effort computations for a set of trials with different weights. In each case the weight at the hand was projected into joint space and added to the gravity vector associated with the limb segments. The arm configurations at the targets did not

dramatically change with increased weight at the hand. This implies that the subjects tended to generate stereotyped reaching postures that were not highly sensitive to the weight being carried. As a consequence we included a weighting between the component of the gravity vector associated with limb masses and the component associated with the external weight carried at the hand. With this weighting we were able to maintain good predictions with increases in the weight at the hand.

Figure 4. Muscle effort variation for a set of trials to the fourth target location with different weights in hand. The weight at the hand was projected into joint space and added to the gravity vector associated with the limb segments The locations of the subject's chosen configurations are depicted with a red +.

5. Conclusions

Building upon the work of Khatib et al., 2004, we have implemented a new muscle effort criteria for predicting physiologically accurate upper limb motion. This criteria is a generalization of the joint decoupled measure used previously. The new criteria properly accounts for the cross-joint coupling associated with multi-articular muscle routing kinematics. We also employ a new kinematically constrained model of the human shoulder complex (Holzbaur et al., 2005). The modeling of the shoulder rhythm using constraints between the scapula, clavicle, and humerus provides more physiologically accurate muscle routing kinematics and, consequently, better estimates of muscle induced moment arms

about the glenohumeral joint (De Sapio et al., 2006). Through a set of subject trials we have shown good correlation between natural reaching postures and those predicted by our proposed criteria.

## 6.	Acknowledgements

References

de Groot, J. H., and Brand, R. (2001), A three-dimensional regression model of the shoulder rhythm, *Clinical Biomechanics*, vol. 16, pp. 735-743.

De Sapio, V., Warren, J., Khatib, O., and Delp S. (2005), Simulating the Task-level Control of Human Motion: A Methodology and Framework for Implementation, *The Visual Computer*, vol. 21, no. 5, pp. 289-302.

De Sapio, V., Holzbaur, K.R., and Khatib, O. (2006), The Control of Kinematically Constrained Shoulder Complexes: Physiological and Humanoid Examples, *Proceedings of the 2005 IEEE International Conference on Robotics and Automation*, vol. 1, pp. 470-475, Barcelona, April 2005.

Delp, S.L., and Loan, J.P. (2000), A Computational Framework for Simulating and Analyzing Human and Animal Movement, *IEEE Computing in Science and Engineering*, vol. 2, no. 5, pp. 46-55.

Holzbaur, K.R., Murray, W.M., and Delp, S.L. (2005), A Model of the Upper Extremity for Simulating Musculoskeletal Surgery and Analyzing Neuromuscular Control, *Annals of Biomedical Engineering*, vol. 33, no. 6, pp. 829-840.

Kang, T., He, J., Helms Tillery, S.I. (2005), Determining natural arm configuration along a reaching trajectory, *Experimental Brain Research*, vol. 167, pp. 352-361.

Khatib, O., Warren, J., De Sapio, V., and Sentis, L. (2004), Human-like motion from physiologically-based potential energies, Lenarčič, J., Galletti, C.(eds.),*On advances in robot kinematics*, pp. 149-163, Boston: Kluwer, 2004.

Klopčar, N., and Lenarčič, J. (2001), Biomechanical Considerations on the Design of a Humanoid Shoulder Girdle, *Proceedings of the 2001 IEEE/ASME International Conference on Advanced Intelligent Mechatronics*, vol. 1, pp. 255-259, Como, Italy.

Holzbaur, K.R., Murray, W.M., and Delp, S.L. (1982), Coordination of Arm and Wrist Motion During a Reaching Task, *Journal of Neuroscience*, vol. 2, no. 4, pp. 399-408.

Lenarčič, J., Stanišić, M.M., and Parenti-Castelli, V. (2000), Kinematic design of a humanoid robotic shoulder complex, *Proceedings of the 2000 IEEE International Conference on Robotics and Automation*, vol. 1, pp. 27-32, San Francisco, CA.

Soechting, J.F., Buneo, C.A., Herrmann, U., Flanders, M. (1995), Moving Effortlessly in Three Dimensions: Does Donders Law Apply to Arm Movement? *Journal of Neuroscience*, vol. 15, pp. 6271-6280.

Uno, Y., Kawato, M., Suzuki, R. (1989), Formation and control of optimal trajectory in human multijoint arm movement, *Biological Cybernetics*, vol. 61, pp. 89-101.

Zajac, F.E. (1993) Muscle coordination of movement: a perspective, *Journal of Biomechanics*, vol. 26, pp. 109-124.